^{1}H-Localized Broadband ^{13}C NMR Spectroscopy of the Rat Brain In Vivo at 9.4 T

Pierre-Gilles Henry,[1] Ivan Tkáč,[1] and Rolf Gruetter[1,2]*

Localized ^{13}C NMR spectra were obtained from the rat brain in vivo over a broad spectral range (15–100 ppm) with minimal chemical-shift displacement error (<10%) using semi-adiabatic distortionless enhancement by polarization transfer (DEPT) combined with ^{1}H localization. A new gradient dephasing scheme was employed to eliminate unwanted coherences generated by DEPT when using surface coils with highly inhomogeneous B_1 fields. Excellent sensitivity was evident from the simultaneous detection of natural abundance signals for N-acetylaspartate, *myo*-inositol, and glutamate in the rat brain in vivo at 9.4 T. After infusion of ^{13}C-labeled glucose, up to 18 ^{13}C resonances were simultaneously measured in the rat brain, including glutamate C2, C3, C4, glutamine C2, C3, C4, aspartate C2, C3, glucose C1, C6, N-acetyl-aspartate C2, C3, C6, as well as GABA C2, lactate C3, and alanine C3. ^{13}C-^{13}C multiplets corresponding to multiply labeled compounds were clearly observed, suggesting that extensive isotopomer analysis is possible in vivo. This unprecedented amount of information will be useful for metabolic modeling studies aimed at understanding brain energy metabolism and neurotransmission in the rodent brain. Magn Reson Med 50:684–692, 2003. © 2003 Wiley-Liss, Inc.

Key words: polarization transfer; ^{13}C NMR spectroscopy; localization; brain metabolism

^{13}C NMR spectroscopy is a powerful tool to study compartmentalized metabolism in the brain (1). In particular, the measurement of ^{13}C labeling time courses during infusion of ^{13}C-labeled glucose and their analysis with a metabolic model has the potential to yield *quantitative* metabolic fluxes through a number of important pathways, including glycolysis, tricarboxylic acid (TCA) cycle, glutamate-glutamine cycle, pyruvate carboxylase, and malate-aspartate shuttle. Such metabolic modeling becomes more robust as the number of simultaneously detected ^{13}C labeling time courses increases, because fewer assumptions are necessary in the model. Therefore, metabolic modeling studies ideally require *broadband* detection of many metabolites with excellent temporal and spectral resolution.

[1]Department of Radiology, Center for Magnetic Resonance Research, University of Minnesota Medical School, Minneapolis Minnesota.

[2]Department of Neuroscience, Center for Magnetic Resonance Research, University of Minnesota Medical School, Minneapolis Minnesota.

*Correspondence to: Rolf Gruetter, Center for Magnetic Resonance Research, 2021 6th St. SE, Minneapolis, MN 55455. E-mail: gruetter@cmrr.umn.edu

Most initial in vivo NMR studies of rodents using *direct* ^{13}C detection have been performed without localization (2–4). However, localization is desirable to detect spectra from a well-defined region of the brain and to avoid contamination by signals from noncerebral tissue. In addition, the lack of localization in directly detected ^{13}C NMR spectra requires the measurement of a natural abundance background spectrum, introducing potential subtraction errors (due to motion or linewidth changes) as an additional experimental complication and reducing the sensitivity of the experiment. Recently, a nonecho localization method based on ^{13}C outer volume suppression (OVS) provided ^{13}C NMR spectra where doubly labeled isotopomers of glutamate and glutamine could be clearly identified (5). However, direct ^{13}C localization invariably leads to a significant chemical-shift displacement error, especially at high B_0 magnetic field, so that only a portion of the ^{13}C spectrum is usually detected. It is therefore not surprising that localized broadband detection of the entire ^{13}C spectrum has not been achieved using direct localization of the ^{13}C magnetization.

An elegant solution to reduce the chemical-shift displacement error takes advantage of the much smaller range of ^{1}H chemical shifts. In this scheme, localization is performed on the ^{1}H magnetization and the localized magnetization is subsequently transferred to carbon using polarization transfer sequences like distortionless enhancement by polarization transfer (DEPT) (6), INEPT (7), or J-cross-polarization (8). The use of DEPT combined with proton localization was first proposed with a volume coil in phantom experiments (9) and was reported to be feasible when using a surface coil as a transceiver (10). Subsequent studies reported the use of full 3D localization in the human brain in vivo using surface coils (11). Incorporation of adiabatic pulses was shown to improve efficiency of polarization transfer when using surface coils with inhomogeneous RF fields (12,13). Finally, polarization transfer sequences combined with ^{1}H-localization were used to measure ^{13}C-label incorporation in human brain metabolism during ^{13}C-labeled glucose infusion (11,13–16) and in the monkey brain (17). To the best of our knowledge, however, the use of polarization transfer to detect localized ^{13}C NMR spectra has not been reported in the rat brain in vivo.

Therefore, the aims of the present study were: 1) to achieve *localized* and *broadband* detection of ^{13}C NMR spectra in the rat brain with minimum chemical-shift displacement error using polarization transfer; 2) to demonstrate the excellent sensitivity and spectral resolution using this technique at 9.4 T; and 3) to evaluate the possibil-
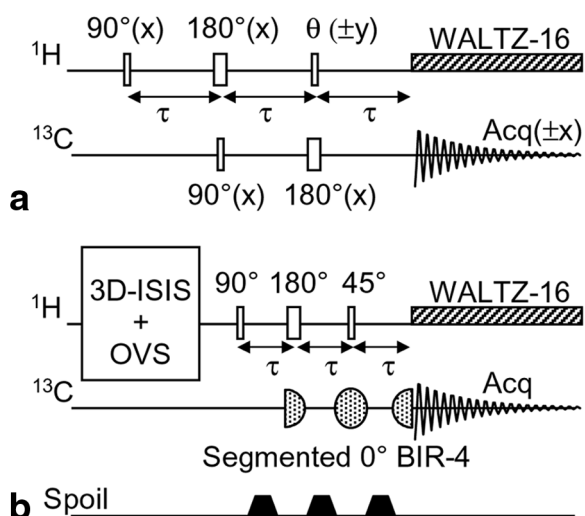
FIG. 1. Semi-adiabatic ¹H-localized polarization transfer. **a:** the original DEPT sequence. **b:** the modified sequence used in the present study. The ¹³C part of DEPT was replaced by a segmented adiabatic 0° BIR-4 pulse. Dephasing gradients (1 ms duration, 46 mT/m) where added between the RF pulses in DEPT to eliminate unwanted, offset-dependent coherences. The flip angle of last ¹H pulse was set to a nominal 45° to detect signals simultaneously from the CH, CH_2, and CH_3 groups.

ity of detecting simultaneously singly and multiply labeled isotopomers in vivo. Overall, these methodological advances resulted in an unprecedented sensitivity and a spectral quality hitherto achievable only in extracts.

THEORY

Gradient-Dephased Semi-adiabatic DEPT Sequence

In principle, the DEPT sequence (6) requires precisely calibrated RF pulses to maximize efficiency and minimize unwanted coherence pathways (Fig. 1a). However, in vivo NMR measurements often use surface coils with inhomogeneous B_1 fields for better sensitivity. In addition, at high B_0 magnetic fields, homogeneous RF fields are difficult to achieve even with volume coils. Under these conditions, well-defined flip angles cannot be obtained over the entire volume of interest using conventional RF pulses, especially if the size of the voxel is comparable to the dimensions of the coil.

The main consequence of imperfect RF pulses is to reduce the polarization transfer efficiency, thereby decreasing the sensitivity of the experiment. To limit signal loss, the ¹³C part of DEPT can be replaced by a segmented 0° BIR-4 (13), resulting in the scheme shown in Fig. 1b. The principal advantage of the added BIR-4 pulse is that the first and second segment of the BIR-4 pulse achieve constant 90° and 180° angles, provided that the adiabatic condition is met (18,19). The last segment is necessary to refocus the nonlinear phase generated by the first two segments. The use of a segmented BIR-4 was particularly advantageous in our study for the ¹³C part of the pulse sequence because of the small size of the ¹³C coil, which resulted in a highly inhomogeneous B_1 field. In contrast, square pulses can be kept for the proton part of DEPT

provided that the B_2 field is reasonably homogeneous over the localized volume, as with the quadrature ¹H coil used in the present study (20).

Another consequence of imperfect RF pulses is the creation of unwanted coherences whose intensity may be dependent on frequency offset. In particular, imperfections in the ¹H 180° refocusing pulse result in a signal intensity that is dependent on the ¹H frequency offset. Indeed, it can be shown (see calculation in Appendix) that if the ¹H refocusing pulse angle is assumed to be 2α (instead of 180°), the resulting coherence after polarization transfer is:

$$\sigma = -S_x + S_x \sin^2(\omega\tau)(1 + \cos 2\alpha) - 2I_zS_y \sin(\omega\tau)\sin 2\alpha.$$

[1]

The first term corresponds to the detected magnetization under ideal condition (i.e., $2\alpha = 180°$). The third term I_zS_y corresponds to antiphase magnetization and is canceled when using ¹H decoupling during the acquisition time. The second term corresponds to detected magnetization that is dependent on the ¹H frequency offset ω when 2α deviates from the nominal 180° value. One well-known remedy to eliminate unwanted coherences generated by imperfect 180° pulses is the EXORCYCLE phase cycle (21). However, because DEPT contains two refocusing pulses, a minimum of 16 phase cycle steps are necessary to eliminate unwanted coherences (10). ISIS localization requires an additional 8 steps phase cycle, resulting in at least 128 steps. Such long phase cycle schemes can be detrimental in vivo because possible movement or linewidth changes can cause imperfect signal cancellation.

Therefore, we propose here to eliminate unwanted coherences by using gradient pulses ("spoilers") during the interpulse delays instead of using phase cycling (Fig. 1b). Because the second gradient pulse acts simultaneously on ¹H and ¹³C transverse coherences, only three gradient pulses are necessary for the two 180° refocusing pulses. The combination of DEPT with gradient spoiling renders phase cycling of either 180° pulse unnecessary, thus reducing the length of the phase cycle scheme by a factor of 16.

Finally, accurate localization requires the elimination of any signal coming from the initial ¹³C magnetization, which does not experience ¹H localization pulses, and is therefore not localized. In the original DEPT sequence, elimination of this directly excited signal was achieved by phase cycling the last proton pulse $\Theta[\pm y]$ together with the receiver $[\pm x]$. In the semi-adiabatic DEPT described here, the 0° BIR-4 returns directly excited ¹³C magnetization back to the z axis. In addition, signal that does not experience the ¹H localization pulses is eliminated by the receiver phase cycle during ISIS. Therefore, it was not necessary to apply a phase cycle to the last ¹H pulse of DEPT in this scheme.

To summarize, the new gradient-dephased semi-adiabatic DEPT sequence proposed in here has been designed to provide accurate 3D localization of ¹³C signals while minimizing sensitivity losses and offset-dependent unwanted coherences generated in the presence of inhomogeneous RF fields, and while minimizing the length of the phase cycle.

MATERIALS AND METHODS

Instrumentation

All experiments were performed on a 9.4T/31cm horizontal bore magnet interfaced to an Inova console (Varian, Palo Alto, CA). The gradient insert (11 cm internal diameter) reached 300 mT/m in 500 μs and was equipped with a customized set of second-order shim coils (Magnex Scientific, Oxford, UK) capable of generating shim fields of 0.01 mT/cm²/A with a 4A shim power supply (Resonance Research, Billerica, MA). The coil assembly consisted of a ¹H quadrature surface coil and a ¹³C linearly polarized surface coil built according to a previously described design (20). The maximum $\gamma B_1/2\pi$ at the coil center was 10 kHz for the ¹³C coil and 6 kHz for the proton coil. To reduce interference between the ¹³C and ¹H channel, two custom-manufactured proton bandpass filters at 400 MHz (Trilithic, Indianapolis, IN) were inserted between each proton coil and the quadrature hybrid and a ¹³C lowpass filter at 100 MHz (Trilithic) was inserted into the ¹³C path between the RF coil and the T/R switch.

Pulse Sequence

In all experiments, multislice RARE images (3 × 3 cm², matrix 256 × 128, 11 slices, TR = 5 sec, TE = 60 ms, 8 echoes per excitation) were used to position the voxel. Localized shimming was performed using FASTESTMAP (22), resulting in an 18–23 Hz full width at half height of the water resonance in a 400 μl voxel (9 × 5 × 9 mm³).

The pulse sequence consisted of ¹H localization followed by semi-adiabatic DEPT (13) (Fig. 1). Localization was performed using 3D-ISIS (hyperbolic secant inversion pulses (23), 2 ms duration, 8 kHz bandwidth) combined with outer volume suppression (OVS). The OVS module consisted of six slice-selective excitation pulses (HS20 (24), bandwidth 42 kHz at 1 ms duration) followed by dephasing gradients. The slice thickness was 15 mm along X (1 ms pulse duration); 15 mm along Z (1.5 ms pulse duration); 12 mm (2 ms pulse duration) and 3.4 mm (1 ms pulse duration) along Y, below and above the voxel, respectively. The carrier frequency was placed at 3.07 ppm for all ¹H localization RF pulses. The shift in voxel position caused by chemical-shift displacement error was largest for the H1 of α-glucose at 5.23 ppm (2.16 ppm frequency offset from the carrier, or 865 Hz at 9.4 T, leading to a displacement error of ~10% of the voxel dimension). Different chemical-shift displacement errors for ISIS and for OVS slices also caused signal loss off-resonance, the effect of which can be calibrated in phantom experiments.

For polarization transfer, the last pulse of DEPT was set to 45° to allow simultaneous detection of CH, CH₂, and CH₃ resonances. Square pulses of duration 50, 100, and 25 μs were used on the ¹H channel for the 90, 180, and 45° pulse, respectively, corresponding to a $\gamma B_1/2\pi$ of 5 kHz. The interpulse delay τ in DEPT was chosen equal to 3.8 ms, optimal for J_{CH} = 130 Hz (only glucose has significantly different J_{CH} values equal to 160–170 Hz as stated previously (25)). The ¹H power was calibrated at the coil center on a sphere containing 99% enriched formic acid (26). This calibration was used to set the optimal ¹H RF power on the voxel based on phantom precalibration measurements at the same voxel position relative to the ¹³C coil center. A segmented 0° BIR-4 (2 ms duration) was used on the ¹³C channel to minimize signal loss due to B_1 inhomogeneity. The carrier frequency was placed at 49.3 ppm for ¹³C and at 3.07 ppm for ¹H. WALTZ-16 composite pulse decoupling was applied during the acquisition time (205 ms, 8192 complex points) with a nominal $\gamma B_1/2\pi$ of 2 kHz. Gradient spoiling (46 mT/m, 1 ms duration) was applied between RF pulses in DEPT to eliminate unwanted coherences. Performance of the sequence and precalibration of ¹H power was determined in a phantom containing 200 mM of 99% enriched [1-¹³C]glucose.

Animal Preparation

Animal experiments were carried out in accordance with the guidelines for the care and use of laboratory animals and were approved by the Institutional Animal Care and Use Committee (IACUC) of the University of Minnesota. Male Sprague-Dawley rats, fasted overnight, were intubated and ventilated with a 70/30 N_2O/O_2 mixture and 1.8% isoflurane. Both femoral veins and femoral arteries were cannulated. The right and left veins were used to infuse glucose and α-chloralose, respectively. Arterial blood was drawn to determine blood gases and plasma glucose concentrations. After completion of surgery, isoflurane was discontinued and replaced by intravenous α-chloralose (bolus 40 mg/kg, then infusion at 25.4 mg/kg/hr). The animal was placed prone in a custom-built stereotaxic holder including a bite-bar and ear barrels. Body temperature was maintained at 37°C with hot water circulation regulated by feedback from a rectal temperature probe. Physiological parameters were maintained within normal limits (pH = 7.35–7.45, pCO_2 = 30–45 mmHg, pO_2 > 100 mmHg) by small adjustments of respiration rate and volume.

Glucose Infusion

After adjustment of NMR parameters, a bolus of 99% enriched ¹³C-labeled glucose was infused i.v. at an exponentially decaying rate over 5 min, followed by a continuous infusion of 70% enriched glucose as previously described (27). This protocol was designed in bench experiments and verified to result in a rapid rise of glucose ¹³C isotopic enrichment from 1.1 to 70%. Plasma glucose was measured every 15–20 min and maintained constant at ~16 mM (corresponding to a brain glucose concentration of 4.5 μmol/g according to Ref. 28) by small adjustments of the glucose infusion rate. ¹³C NMR spectra were collected in blocks of 5.4 min over 7 hr. [1-¹³C]Glucose was purchased from Isotec (Miamisburg, OH); [1,6-¹³C₂]glucose from Cambridge Isotope Laboratories (Andover, MA); and [U-¹³C₆]glucose from Martek (Columbia, MD).

Data Processing

NMR signals were averaged and saved on disk in blocks of 128 scans (repetition time 2.5 sec) corresponding to an acquisition time of 5.4 min. Spectra averaged over longer periods of time were obtained by adding 5.4 min blocks after frequency correction to correct for the drift of the B_0 magnetic field. The frequency drift was determined using
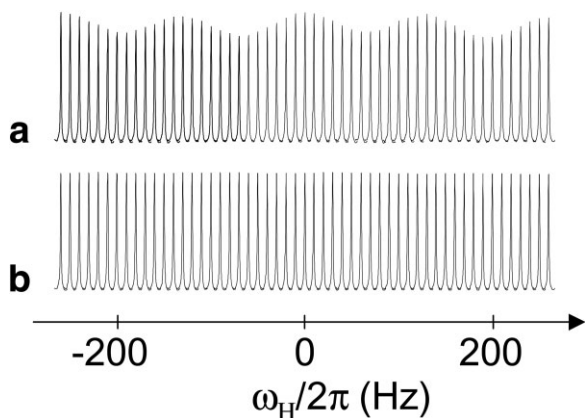
FIG. 2. Decoupler off-resonance effects of polarization transfer when using a surface coil as a transceiver. The C1 resonance of β-D-glucose at 96.7 ppm was measured as a function of the ¹H decoupler offset (10 Hz increments) in a phantom containing 200 mM of 99% enriched [1-¹³C]glucose using the sequence depicted in Fig. 1b. **a:** *Without* gradient spoiling, the detected signal oscillates as a function of ¹H frequency offset. **b:** *With* gradient spoiling, oscillations are suppressed.

the glutamate C4 peak at 34.4 ppm and frequency correction was applied directly in the time domain. For natural abundance spectra, no frequency correction was used. Fourier transform was performed with filtering parameters specified in the figure captions. No baseline correction was applied.

RESULTS

The elimination of off-resonance effects induced by semi-adiabatic polarization transfer in inhomogeneous RF fields was validated in phantom studies. As expected from the theoretical analysis (Eq. [1]), the use of DEPT with a surface coil resulted in an oscillating excitation profile when the decoupler ¹H frequency was varied (Fig. 2a). These oscillations were completely suppressed by gradient spoiling (Fig. 2b). This demonstrates the efficiency of gradient spoiling to eliminate unwanted pathways generated by imperfect RF pulses.

Spectra acquired in the rat brain in vivo using the sequence depicted in Fig. 1b showed substantial sensitivity gains compared to previous localized ¹³C NMR studies of rat brain (5,29) (Fig. 3). For example, natural abundance
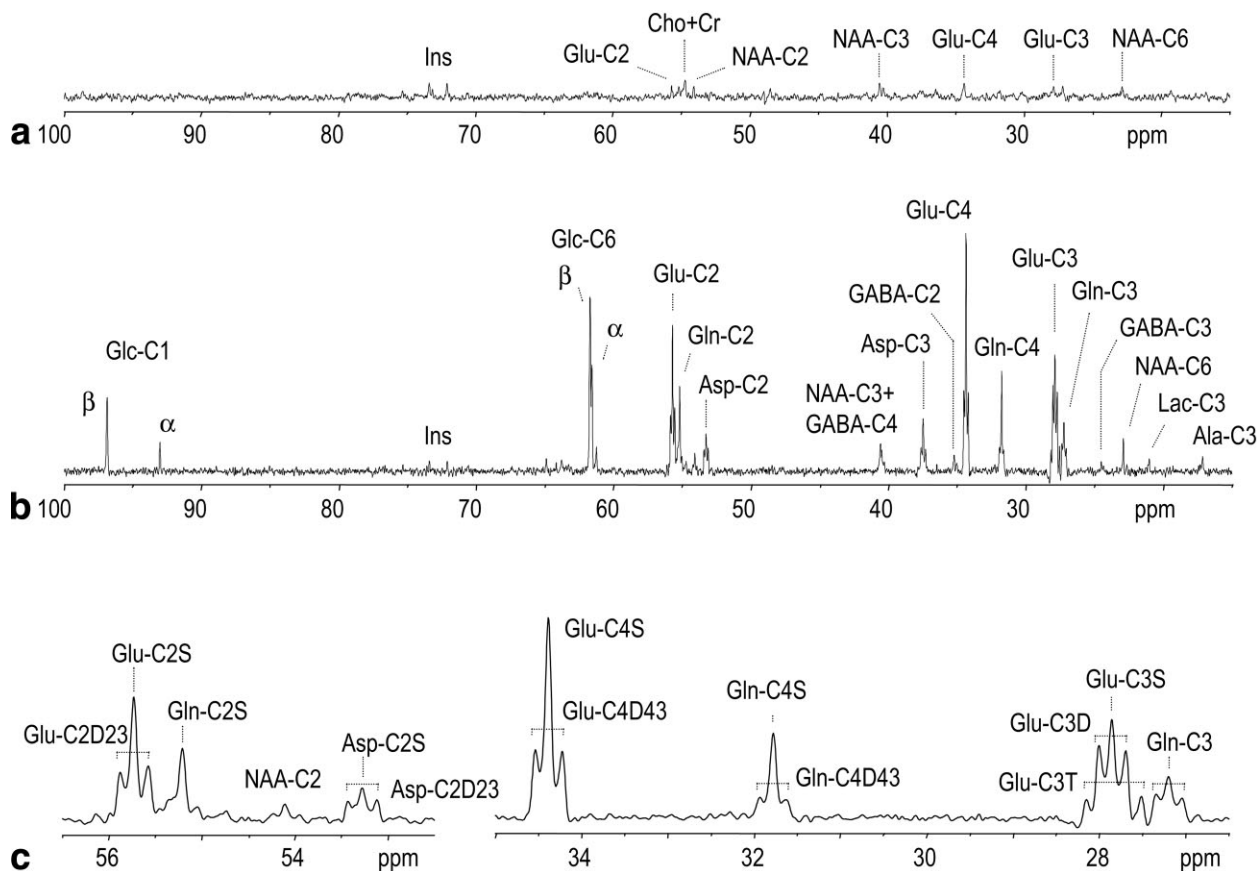

FIG. 3. In vivo ¹³C spectra from a 400 μl volume in the rat brain, acquired using the modified DEPT sequence depicted in Fig. 1b. **a:** Natural abundance spectrum acquired for 3.5 hr (5120 scans, TR 2.5 sec). **b:** Spectrum recorded for 1.8 hr (2560 scans, TR = 2.5 sec) during an infusion of 70% enriched [1,6-¹³C₂]glucose. Acquisition was started 1.8 hr after the beginning of glucose infusion. **c:** Expansion of **b** showing the detection of doubly labeled isotopomers of glutamate, glutamine, and aspartate. Note the triplet of glutamate (Glu-C3T) at 27.9 ppm, corresponding to glutamate labeled simultaneously at the C2, C3, and C4 positions. Processing consisted of zero-filling, filtering (5 Hz Lorentzian line broadening for (**a**) and 2 Hz Lorentzian-to-Gaussian resolution enhancement for (**b**) and (**c**)), and fast Fourier transform. No baseline correction was applied.

^{13}C NMR signals of metabolites were detected for the first time in the rat brain (Fig. 3a). Several resonances from natural abundance glutamate, *myo*-inositol, and NAA (corresponding to a ^{13}C concentration of ~0.1 μmol/g) were clearly observed. Reliable localization of the NMR signals to the brain over the entire spectral range of 8 kHz was evident from the complete absence of lipid signal at 30 ppm, of lipid glycerol resonances at 61 and 69 ppm, and of olefinic carbon resonances at 130 ppm, all of which arise from skin and muscles surrounding the brain. After infusion of [1,6-^{13}C$_2$]glucose, up to 18 resonances were detected (Fig. 3b). These included signals from the C1 of α- and β-glucose at 92.9 and 97.8 ppm, the C6 of α- and β-glucose at 61.7 and 61.8 ppm, and signals from all CH$_n$ resonances of glutamate (at 55.9, 34.4, and 27.9 ppm), glutamine (at 55.2, 31.9, and 27.1 ppm), and aspartate (at 53.2 and 37.5 ppm). In addition, weaker resonances from NAA, GABA, alanine, and lactate were detected.

The linewidth of ^{13}C singlet resonances were typically 5–6 Hz (0.05 ppm). The high spectral resolution in the spectrum can be appreciated from the observation that the signals from the C6α and C6β glucose resonances were resolved in vivo despite a chemical shift difference of only 0.14 ppm (14 Hz at 9.4T). An expansion of the spectral region at 55 ppm and at 30 ppm (Fig. 3c) shows that with such a narrow linewidth the fine structure due to ^{13}C-^{13}C couplings was readily observed. For example, the glutamate C3 resonance at 27.9 ppm is a superposition of a singlet (Glu-C3S), a doublet (Glu-C3D), and a triplet (Glu-C3T). The detection of these multiply labeled amino acids following infusion of [1-^{13}C] or [1,6-^{13}C$_2$] glucose reflected the cycling of ^{13}C label through the TCA cycle.

Comparing the effect of infusing [1-^{13}C]glucose, [1,6-^{13}C$_2$]glucose, and [U-^{13}C]glucose (all infused with a fixed isotopic enrichment of 70%) on the detection of the ^{13}C-^{13}C isotopomers of glutamate and glutamine clearly indicated a strong influence of the type of ^{13}C-labeled precursor being administered (Fig. 4). With [1-^{13}C]glucose (Fig. 4a), the spectrum was dominated by singlets, with small contributions from the doublets. After infusion of [1,6-^{13}C$_2$]glucose (Fig. 4b), the relative proportion of multiplets in glutamate and glutamine compared to the singlets was increased due to the expected 2-fold increase in the isotopic enrichment of [2-^{13}C]acetyl-CoA entering the TCA cycle. In this case, a triplet, Glu-C3T, was clearly detected at 27.9 ppm. Lastly, when infusing [U-^{13}C$_6$]glucose (Fig. 4c), the glutamate and glutamine C4 resonances were further split by the coupling (J$_{45}$ = 53 Hz) to the C5 (carboxyl) carbons in glutamate and glutamine which were labeled from the C2 and C5 carbons of glucose.

Using the proposed methodology, labeling time courses of many resonances were detected simultaneously in the same animal over extended periods of time at a high temporal resolution of 5 min (Fig. 5a). During 7 hr of infusion of [1,6-^{13}C2]glucose, glutamate C4 was labeled first along with the C2 and C3 of aspartate, followed by glutamine C4 and the C2 and C3 carbons of glutamate and glutamine. We also noted the labeling of the NAA C2, C3, and C6 resonances at a much slower rate (Fig. 5b), as well as the detection of label in the GABA C2, C3, and C4 resonances with a lower temporal resolution (not shown).
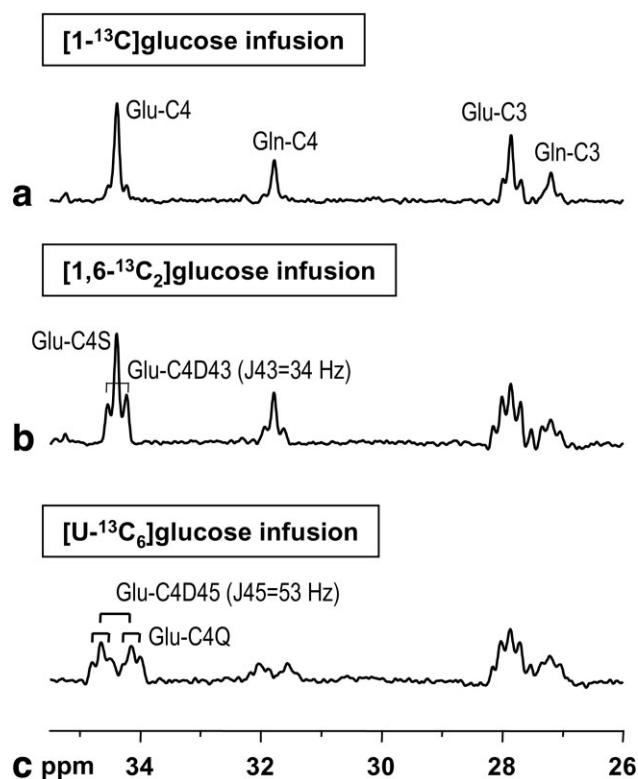

FIG. 4. Effect of the infused substrate on the labeling pattern. Shown are the spectral regions containing glutamate and glutamine C4 and C3 in vivo after infusion of (**a**) [1-^{13}C]glucose, (**b**) [1,6-^{13}C$_2$]glucose, and (**c**) [U-^{13}C$_6$]glucose (volume 400 μl). The isotopic enrichment of the infusate was 70% in all cases. Each spectrum corresponds to 1.8 hr of acquisition (2560 scans, TR = 2.5 sec) started 4.5 hr after the beginning of glucose infusion. Mild Lorentzian-to-Gaussian resolution enhancement was used.

The improved sensitivity was used to detect ^{13}C label in smaller volumes of 48 μl matched to the somatosensory cortex (Fig. 6). Resonances from glucose C6, glutamate C2, C3, C4, and glutamine C2, C3, C4, and aspartate C2, C3 were readily detected in 11 min, indicating the feasibility of combining time-resolved direct-detected ^{13}C spectroscopy with functional activation of somatosensory cortex in the rat brain.

DISCUSSION

This study demonstrates that efficient localization covering the entire range of ^{13}C resonances can be achieved in the rat brain in vivo. The chemical-shift displacement was minimized by using proton localization followed by polarization transfer, taking advantage of the smaller chemical-shift range of ^{1}H spectra. For most detected metabolites, such as glutamate, glutamine, NAA, aspartate, and GABA, whose proton chemical-shift falls in the range 1.9–4.3 ppm, the chemical-shift displacement error was less than 6% of the voxel dimension in each spatial direction. The largest chemical-shift displacement error occurred for the H1 of α-glucose at 5.23 ppm and did not exceed 10% of the voxel dimension. Accurate localization over the entire spectral range was evident from the complete absence of
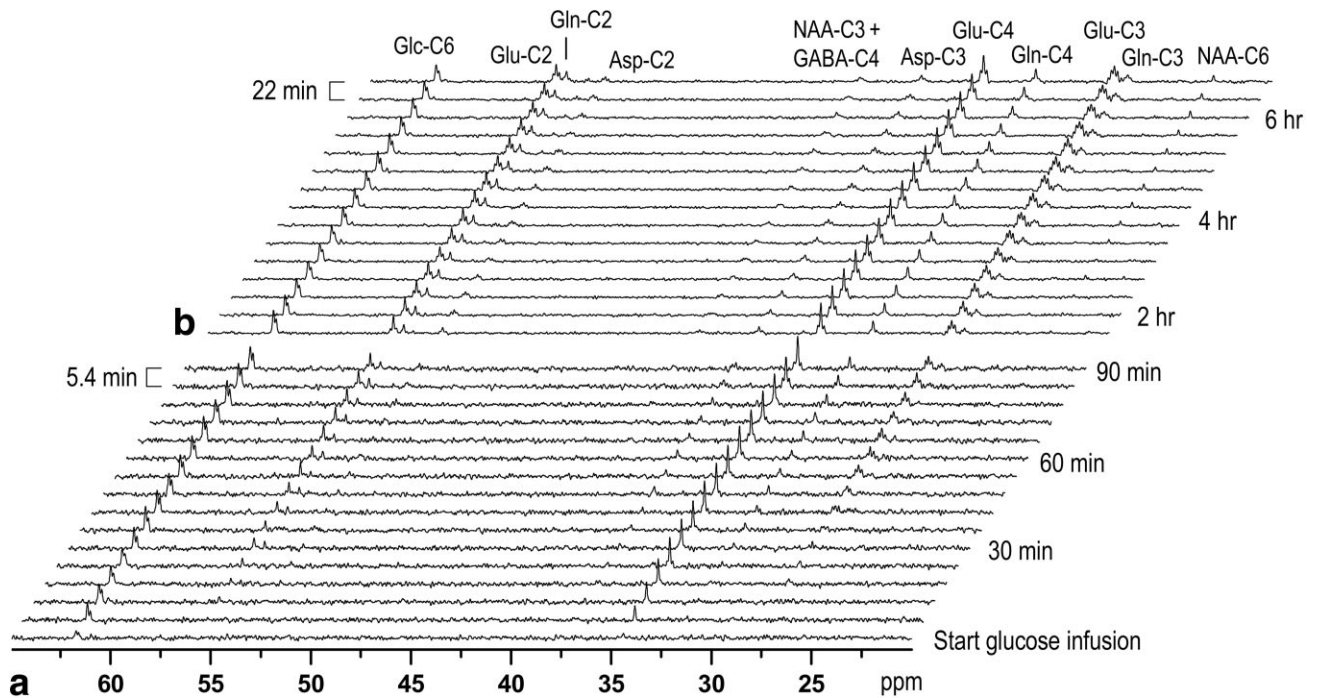
FIG. 5. Time course of ¹³C label incorporation during an infusion of [1,6-¹³C₂]glucose. The stack plot of an expansion of the ¹³C spectra shows (**a**) the first 90 min with a temporal resolution of 5.4 min (128 scans each, TR = 2.5 sec), showing label incorporation into glucose C6, glutamate C4, C3, C2, glutamine C4, C3, C2, and aspartate C2 and C3; (**b**) the subsequent 5.5 hr with a temporal resolution of 22 min, showing the slower labeling of NAA C2, C3, and C6. Mild Lorentzian-to-Gaussian resolution enhancement was applied.

lipid signals at 30, 63, and 69 ppm, as well as the elimination of the olefinic carbon resonances at 130 ppm (not shown), all of which arise from surrounding adipose and muscle tissues.

For the localization of carbon resonances with small or absent coupling to protons ($J_{CH} \sim 0$) such as the carboxyl resonances around 180 ppm (e.g., the C1 and C5 of glutamate), obviously polarization transfer cannot be used and localization methods
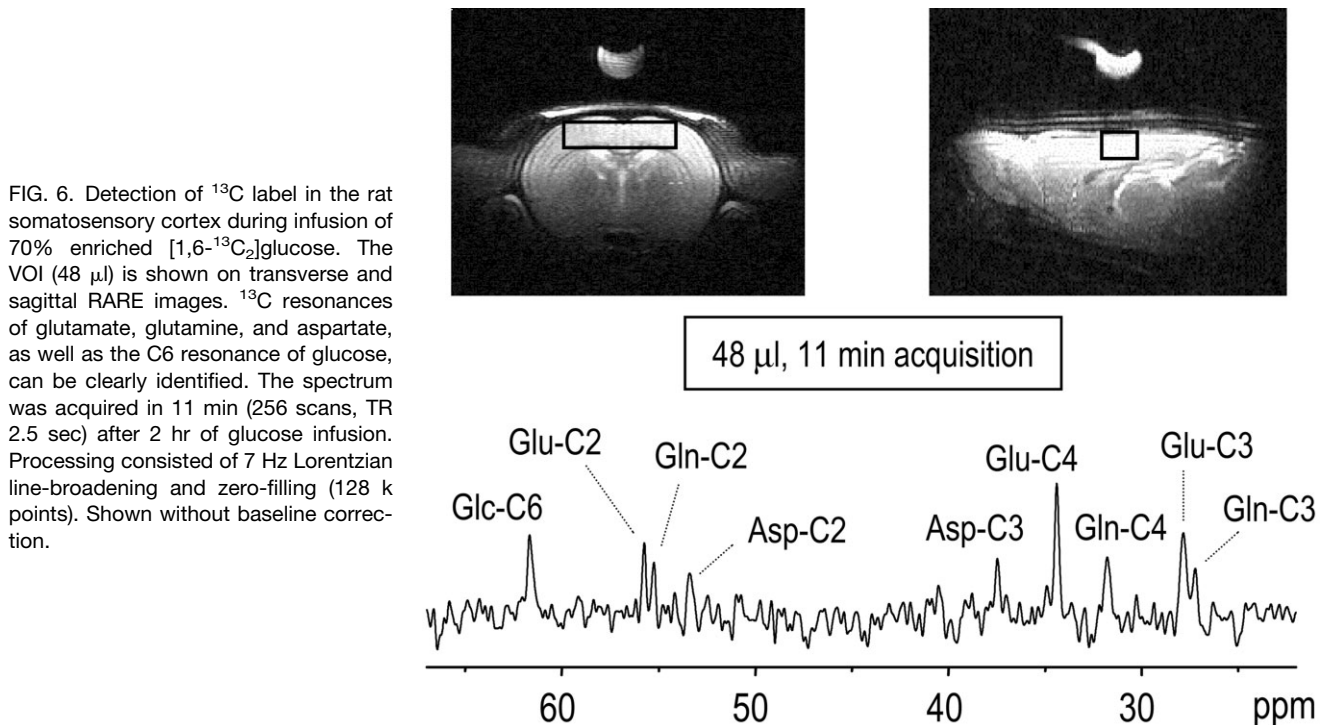

FIG. 6. Detection of ¹³C label in the rat somatosensory cortex during infusion of 70% enriched [1,6-¹³C₂]glucose. The VOI (48 μl) is shown on transverse and sagittal RARE images. ¹³C resonances of glutamate, glutamine, and aspartate, as well as the C6 resonance of glucose, can be clearly identified. The spectrum was acquired in 11 min (256 scans, TR 2.5 sec) after 2 hr of glucose infusion. Processing consisted of 7 Hz Lorentzian line-broadening and zero-filling (128 k points). Shown without baseline correction.

based on the ^{13}C magnetization are required, like outer volume suppression (5) or ISIS (30). ^{13}C resonances with very short relaxation times are also not easily detected using polarization transfer methods (due to relaxation during polarization transfer) and nonecho localization methods have been proposed for the measurement of glycogen (5).

Although polarization transfer greatly reduced the chemical-shift displacement error, deviations of the RF pulses from the nominal flip angle resulted in less than maximal efficiency and selection of unwanted coherence transfer pathways. In particular, an imperfect ^1H 180° RF pulse created unwanted coherences that resulted in an excitation profile that oscillated as a function of ^1H frequency offset (Fig. 2a). Precise calibration of RF pulses can be achieved even with surface coils, provided that the RF field remains reasonably homogeneous across the voxel chosen for spectroscopy (11,13). Alternatively, if this cannot be achieved, e.g., when the voxel dimensions are large compared to the coil, as was the case in the present study, unwanted coherences can be eliminated by phase cycling the 180° refocusing pulses for both nuclei (10). However, significant signal loss can occur in regions where the flip angles deviate from their nominal value. To optimize sensitivity, we replaced the ^{13}C part of DEPT by a segmented 0° BIR-4. This resulted in optimal pulse angles for the ^{13}C channel and eliminated the need for precise ^{13}C power calibration, which was critical given the small size of the ^{13}C coil (11 mm diameter). We furthermore introduced the use of dephasing gradients to eliminate the need for phase cycling 180° pulses on either ^{13}C or ^1H channels, thereby greatly reducing the number of steps in the phase cycle.

The combination of ^1H localization and polarization transfer at 9.4 T resulted in the *localized* detection of the entire ^{13}C spectrum (with the exception of resonances from carbons that have no proton attached, such as carboxyl COOH groups) with excellent sensitivity, as demonstrated by the first simultaneous detection of natural abundance signals of NAA, glutamate and *myo*-inositol in the rat brain in vivo as illustrated in Fig. 3a. The C1,3 resonance of *myo*-inositol was detected at 72.1 ppm in Fig. 3a with a signal-to-rms noise ratio of 5, consistent with the fact that natural abundance signals were observed routinely in the rat brain in vivo in less than 1 hr. The use of one of the highest B_0 fields available to date for this type of in vivo studies was certainly an important factor contributing to the increased sensitivity. Another important element was the combination of a circularly polarized ^1H coil and a linearly polarized ^{13}C coil used (20), which retained a high sensitivity for ^{13}C combined with a relatively homogeneous B_2 field for ^1H localization, decoupling, and polarization transfer. Finally, optimal adjustment of all first- and second-order shims using an automated procedure such as FAST(EST)MAP (22) was crucial to attain optimal sensitivity and spectral resolution, especially at high B_0 magnetic field and for the larger volumes used in ^{13}C NMR (31).

After infusion of ^{13}C-labeled glucose, the new sequence allowed for the simultaneous *localized* detection of up to 18 resonances ranging from glucose C1 to lactate C3 over an 80 ppm bandwidth. This represents a substantial improvement over previous studies using ^{13}C detection in the rat brain, which either measured the whole spectrum without localization (3,4), or detected signal from a smaller spectral range with localization (5).

The excellent sensitivity and spectral resolution further resulted in the detection of multiply labeled metabolites (isotopomers) appearing in the spectrum as multiplets. Spectral resolution has been shown to increase with a higher magnetic field B_0 due to increased chemical-shift dispersion (32). Again, excellent shimming was necessary to resolve homonuclear couplings, as these decrease (when expressed in ppm) with B_0. In the present study a ^{13}C linewidth of 5–6 Hz was routinely achieved for a 400 µl volume. This linewidth was at most 2 Hz above the achievable minimum in rat brain due to residual higher-order shim terms ($n \geq 3$) as estimated from the line width of water in this volume. Nonetheless, such a small linewidth allowed the routine detection of the ^{13}C-^{13}C coupled resonances with J-coupling constants ranging from 31–54 Hz, as illustrated in Figs. 3 and 4. Many studies, especially in brain extracts (33–37) and in the perfused heart (38,39), have shown the usefulness of isotopomer analysis to investigate metabolic pathways and substrate selection. Our results suggest that isotopomer analysis is now feasible in vivo in the rat brain for several metabolites, including glutamate, glutamine, and aspartate, provided that adequate fitting methods are used.

The localization performance, sensitivity, and spectral resolution demonstrated in the present study are expected to considerably extend the scope of ^{13}C NMR studies in the rat brain and animal brain in general. For example, in vivo metabolic studies of the brain to date have used only a fraction of the information potentially available in the ^{13}C spectrum. Measurements have generally focused on one (typically glutamate C4) or two labeling time courses, be it glutamate C4 and glutamate C3 without measuring glutamine (40), or glutamate C4 and glutamine C4 without measuring the C3 (4). In contrast, the detection of time-resolved ^{13}C labeling time courses of more than 15 resonances in vivo is likely to provide a much more comprehensive assessment of metabolism than previously achieved, together with a potential reduction in the number of assumptions in the metabolic modeling. Recent reports have emphasized the importance of including sufficient information in the metabolic modeling to derive quantitative metabolic fluxes (14,27,29). For example, measuring the C3 labeling time course of glutamate and glutamine, in addition to the C4 time course, allows the measurement of the exchange rate between 2-oxoglutarate and glutamate, V_x. A number of recent studies have shown that V_x is most likely slow in the brain, on the order of the TCA cycle flux, and may change with the level of brain activity. In addition, the detection of the C2 labeling time course of glutamine can be used to determine the rate of anaplerosis through pyruvate carboxylase. The detection of aspartate and GABA provide additional information that will be of primary importance to further investigate metabolic compartmentation. In addition, the feasibility to detect ^{13}C labeling in the rat somatosensory cortex (Fig. 6) emphasizes the possibility to measure multiple ^{13}C labeling time courses during functional activation.

CONCLUSION

In conclusion, localized, broadband ^{13}C NMR spectroscopy at high magnetic field can detect ^{13}C resonances over an 80 ppm bandwidth with less than 10% chemical-shift displacement error when using ^{1}H-localization combined with polarization transfer. Excellent sensitivity and spectral resolution was achieved at 9.4 T in the rat brain. We conclude that metabolic information is now accessible in vivo that hitherto had to be obtained in extracts and that numerous labeling time courses in the brain during an infusion of a ^{13}C-labeled substrate can be measured simultaneously in small, functionally specialized areas of the brain. These results enhance the role of ^{13}C NMR spectroscopy as a valuable tool to further investigate models of brain metabolism and compartmentation in health, activation, and disease.

ACKNOWLEDGMENTS

APPENDIX

Effect of an Imperfect 180° Refocusing Pulses in DEPT

The following calculation shows that an imperfect ^{1}H 180° refocusing pulse in DEPT results in a signal that oscillates as a function of the ^{1}H decoupler frequency offset. To simplify the calculation, an AX spin system was considered and all pulses were assumed to be at their nominal angle, except for the proton 180° pulse, for which the flip angle was set to 2α. The ^{13}C observed frequency was assumed to be on resonance (no chemical-shift evolution at carbon frequency) and the effect of homonuclear coupling, J_{HH}, coupling was neglected. The last ^{1}H pulse of DEPT (Θ) was set to the optimal value of 90° for the AX system.

The first proton 90° pulse tilts the initial I_z magnetization to the transverse plane:

$$\sigma = -I_y. \qquad [A1]$$

The magnetization evolves under ^{1}H chemical-shift (ω) and J-coupling during the first delay $\tau = 1/2\,J$:

$$\sigma = 2I_xS_z \cos(\omega\tau) + 2I_yS_z \sin(\omega\tau) \qquad [A2]$$

after the first ^{13}C 90° pulse (Fig. 1a) this coherence is converted to:

$$\sigma = -2I_xS_y \cos(\omega\tau) - 2I_yS_y \sin(\omega\tau) \qquad [A3]$$

and the application of the nominal 180° pulse, assumed here to be 2α, results in:

$$\sigma = -2I_xS_y \cos(\omega\tau) - 2I_yS_y \sin(\omega\tau)\cos 2\alpha$$
$$- 2I_xS_y \sin(\omega\tau)\sin 2\alpha. \qquad [A4]$$

Evolution under chemical-shift and J-coupling during the second delay τ gives:

$$\sigma = \cos(\omega\tau)[-2I_xS_y \cos(\omega\tau) - 2I_xS_y \sin(\omega\tau)]$$
$$+ \sin(\omega\tau)\cos 2\alpha[-2I_yS_y \cos(\omega\tau) + 2I_xS_y \sin(\omega\tau)]$$
$$+ S_x\sin(\omega\tau)\sin 2\alpha = 2I_xS_y[-\cos^2(\omega\tau) + \sin^2(\omega\tau)\cos 2\alpha]$$
$$+ 2I_yS_y[-\cos(\omega\tau)\sin(\omega\tau)(1 + \cos 2\alpha)] + S_x \sin(\omega\tau)\sin 2\alpha.$$
$$[A5]$$

Following the 90°_y pulse, the multiple-quantum term I_yS_y leads to undetectable magnetization and was not further considered in the calculation. Finally, inversion by the 180° ^{13}C pulse and J-coupling evolution during the last delay τ results in Eq. [1]:

$$\sigma = -S_x + S_x \sin^2(\omega\tau)(1 + \cos 2\alpha) - 2I_zS_y \sin(\omega\tau)\sin 2\alpha$$

REFERENCES

1. Gruetter R. In vivo 13C NMR studies of compartmentalized cerebral carbohydrate metabolism. Neurochem Int 2002;41:143–154.
2. Behar KL, Petroff OAC, Prichard JW, Alger JR, Shulman RG. Detection of metabolites in rabbit brain by ^{13}C NMR spectroscopy following administration of [1-^{13}C]Glucose. Magn Reson Med 1986;3:911–920.
3. Sibson NR, Dhankhar A, Mason GF, Behar KL, Rothman DL, Shulman RG. In vivo ^{13}C NMR measurements of cerebral glutamine synthesis as evidence for glutamate-glutamine cycling. Proc Natl Acad Sci USA 1997;94:2699–2704.
4. Sibson NR, Dhankhar A, Mason GF, Rothman DL, Behar KL, Shulman RG. Stoichiometric coupling of brain metabolism and glutamatergic neuronal activity. Proc Natl Acad Sci USA 1998;95:316–321.
5. Choi IY, Tkac I, Gruetter R. Single-shot, three-dimensional "non-echo" localization method for in vivo NMR spectroscopy. Magn Reson Med 2000;44:387–394.
6. Doddrell DM, Pegg DT, Bendall MR. Distortionless enhancement of NMR signals by polarization transfer. J Magn Reson 1982;48:323–327.
7. Morris GA, Freeman R. Enhancement of nuclear magnetic resonance signals by polarization transfer. J Am Chem Soc 1979;101:760–762.
8. Bearden DW, Brown LR. Heteronuclear isotropic mixing in liquids. Chem Phys Lett 1989;163:432–436.
9. Aue WP, Muller S, Seelig J. Localized ^{13}C NMR spectra with enhanced sensitivity obtained by volume-selective excitation. J Magn Reson 1985;61:392–395.
10. Beckmann N, Muller S. Analysis of localized polarization transfer for ^{13}C volume selective spectroscopy with surface coils. J Magn Reson 1991;93:299–318.
11. Gruetter R, Adriany G, Merkle H, Andersen PM. Broadband decoupled, ^{1}H-localized ^{13}C MRS of the human brain at 4 Tesla. Magn Reson Med 1996;36:659–664.
12. Merkle H, Wei H, Garwoord M, Ugurbil K. B_1-insensitive heteronuclear adiabatic polarization transfer for signal enhancement. J Magn Reson 1992;99:480–494.
13. Gruetter R, Seaquist ER, Kim S, Ugurbil K. Localized in vivo ^{13}C-NMR of glutamate metabolism in the human brain: initial results at 4 Tesla. Dev Neurosci 1998;20:380–388.
14. Gruetter R, Seaquist ER, Ugurbil K. A mathematical model of compartmentalized neurotransmitter metabolism in the human brain. Am J Physiol 2001;281:E100–E112.
15. Shen J, Petersen KF, Behar KL, Brown P, Nixon TW, Mason GF, Petroff OAC, Shulman GI, Shulman RG, Rothman DL. Determination of the rate of the glutamate/glutamine cycle in the human brain by in vivo ^{13}C NMR. Proc Natl Acad Sci USA 1999;96:8235–8240.
16. Watanabe H, Umeda M, Ishihara Y, Okamoto K, Oshio K, Kanamatsu T, Tsukada Y. Human brain glucose metabolism mapping using multislice 2D ^{1}H-^{13}C correlation HSQC spectroscopy. Magn Reson Med 2000;43:525–533.
17. Watanabe H, Ishihara Y, Okamoto K, Oshio K, Kanamatsu T, Tsukada Y. 3D localized 1H–13C heteronuclear single-quantum coherence correlation spectroscopy in vivo. Magn Reson Med 2000;43:200–210.
18. Garwood M, Ke Y. Symmetric pulses to induce arbitrary flip angles with compensation for RF inhomogeneity and resonance offsets. J Magn Reson 1991;94:511–525.

19. Kim S-G, Garwood M. Double DEPT using adiabatic pulses. Indirect heteronuclear T_1 measurement with B_1 insensitivity. J Magn Reson 1992;99:660−667.

20. Adriany G, Gruetter R. A half-volume coil for efficient proton decoupling in humans at 4 Tesla. J Magn Reson 1997;125:178−184.

21. Bodenhausen G, Freeman R, Turner DL. Suppression of artifacts in two-dimensional J-spectroscopy. J Magn Reson 1977;27:511−514.

22. Gruetter R, Tkac I. Field mapping without reference scan using asymmetric echo-planar techniques. Magn Reson Med 2000;43:319−323.

23. Silver MS, Joseph RI, Chen C-N, Sank VJ, Hoult DI. Selective population inversion in NMR. Nature 1984;310:681−683.

24. Tannus A, Garwood M. Improved performance of frequency-swept pulses using offset-independent adiabaticity. J Magn Reson A 1996; 120:133−137.

25. Pfeuffer J, Tkac I, Choi I-Y, Merkle H, Ugurbil K, Garwood M, Gruetter R. Localized in vivo ^{1}H NMR detection of neurotransmitter labeling in rat brain during infusion of [1-^{13}C] D-glucose. Magn Reson Med 1999; 41:1077−1083.

26. Bax A. A simple method for the calibration of the decoupler radiofrequency field strength. J Magn Reson 1983;52:76−80.

27. Henry P-G, Lebon V, Vaufrey F, Brouillet E, Hantraye P, Bloch G. Decreased TCA cycle rate in the rat brain after acute 3-NP treatment measured by in vivo ^{1}H-[^{13}C] NMR spectroscopy. J Neurochem 2002; 82:857−866.

28. Choi I-Y, Lee S-P, Kim S-G, Gruetter R. In vivo measurements of brain glucose transport using the reversible Michaelis-Menten model and simultaneous measurements of cerebral blood flow changes during hypoglycemia. J Cereb Blood Flow Metab 2001;21:653−663.

29. Choi IY, Lei HX, Gruetter R. Effect of deep pentobarbital anesthesia on neurotransmitter metabolism in vivo: on the correlation of total glucose consumption with glutamatergic action. J Cereb Blood Flow Metab 2002;22:1343−1351.

30. Gruetter R, Rothman DL, Novotny EJ, Shulman RG. Localized 13C NMR spectroscopy of myo-inositol in the human brain in vivo. Magn Reson Med 1992;25:204−210.

31. Gruetter R. Automatic, localized in vivo adjustment of all first-order and second-order shim coils. Magn Reson Med 1993;29:804−811.

32. Gruetter R, Weisdorf SA, Rajanayagan V, Terpstra M, Merkle H, Truwit CL, Garwood M, Nyberg SL, Ugurbil K. Resolution improvements in in vivo 1H NMR spectra with increased magnetic field strength. J Magn Reson 1998;135:260−264.

33. Cerdan S, Kunnecke B, Seelig J. Cerebral metabolism of [1,2-13C2]acetate as detected by in vivo and in vitro 13C NMR. J Biol Chem 1990;265:12916−12926.

34. Lapidot A, Gopher A. Cerebral metabolic compartmentation. Estimation of glucose flux via pyruvate carboxylase/pyruvate dehydrogenase by 13C NMR isotopomer analysis of D-[U-13C]glucose metabolites. J Biol Chem 1994;269:27198−27208.

35. Hassel B, Sonnewald U, Fonnum F. Glial-neuronal interactions as studied by cerebral metabolism of [2-13C]acetate and [1-13C]glucose: an ex vivo 13C NMR spectroscopic study. J Neurochem 1995;64:2773−2782.

36. Bachelard H. Landmarks in the application of 13C-magnetic resonance spectroscopy to studies of neuronal/glial relationships. Dev Neurosci 1998;20:277−288.

37. Zwingmann C, Richter-Landsberg C, Leibfritz D. 13C isotopomer analysis of glucose and alanine metabolism reveals cytosolic pyruvate compartmentation as part of energy metabolism in astrocytes. Glia 2001;34:200−212.

38. Jeffrey FM, Storey CJ, Sherry AD, Malloy CR. 13C isotopomer model for estimation of anaplerotic substrate oxidation via acetyl-CoA. Am J Physiol 1996;271:E788−799.

39. Malloy CR, Sherry AD, Jeffrey FM. Analysis of tricarboxylic acid cycle of the heart using 13C isotope isomers. Am J Physiol 1990;259:H987−995.

40. Mason GF, Rothman DL, Behar KL, Shulman RG. NMR determination of the TCA cycle rate and α-ketoglutarate/glutamate exchange rate in rat brain. J Cereb Blood Flow Metab 1992;12:434−447.